MODULO EVENT-DRIVEN SAMPLING: SYSTEM IDENTIFICATION AND HARDWARE EXPERIMENTS

Dorian Florescu and Ayush Bhandari

Dept. of Electrical and Electronic Engg., Imperial College London, SW72AZ, UK.
Email: d.florescu@imperial.ac.uk • a.bhandari@imperial.ac.uk

ABSTRACT

In event-driven sampling (EDS) the signal is represented in terms of a series of spikes at non-uniform time locations. Owing to the limited dynamic range (DR), just like how conventional analog-to-digital converters (ADC) suffer from signal saturation, in EDS a similar manifestation is observed. Namely, when the input exceeds a threshold, no output spikes are generated. Recently, the Unlimited Sensing Framework (USF) was presented to overcome the DR limitation. In USF, the key idea is to fold the signal using a modulo non-linearity so that its DR is fixed. Subsequently, we combined EDS with USF leading to a new architecture called Modulo Event-Driven Sampling (MEDS), where a modulo signal is input to the EDS model. The goal of this work is to bridge the gap between theory and practice for a MEDS model. Our hardware experiments suggest that for the MEDS approach to work, there are system parameters that must be identified beforehand so that accurate reconstruction of the input is possible. To this end, we introduce a system identification methodology for MEDS that is backed by theoretical guarantees. Using synthetic and experimental data, we validate the performance of our approach, thus demonstrating the utility of system identification.

***Index Terms*—** Analog-to-digital converter (ADC), sampling theory, modulo samples, time encoding, system identification.

1. INTRODUCTION

Event-driven sampling (EDS) is an alternative acquisition protocol that parallels Shannon's paradigm. Instead of working with pointwise samples, the basis of EDS is the principle of *time encoding*. As the name suggests, in EDS, informative "events" are generated to represent a continuous-time signal; this is inspired from the signal representation in mammalian nervous systems [1]. The EDS paradigm has contributed to new results in sampling theory [2–6] and has inspired new sensing technology such as *event cameras* [7] and *low-power* analog-to-digital converters (ADCs) [8].

Despite the progress on the conceptual frontier of event-driven representation, both in control theory [9] and signal processing [10, 11], the practical implementation of the time encoding paradigm suffers from the same fundamental bottleneck as uniform sampling in Shannon's paradigm. That is, the input signal dynamic range (DR) is constrained by an upper-bound λ. While in the case of uniform sampling ADCs saturate when the input is larger than λ, in the EDS framework the same scenario manifests in a null output [2, 12].

This research is supported by the UK Research and Innovation council's Future Leaders Fellowship program "Sensing Beyond Barriers" (MRC Fellowship award no. MR/S034897/1). Upcoming materials related to *reproducible research* will be available via `https://bit.ly/USF-Link`.

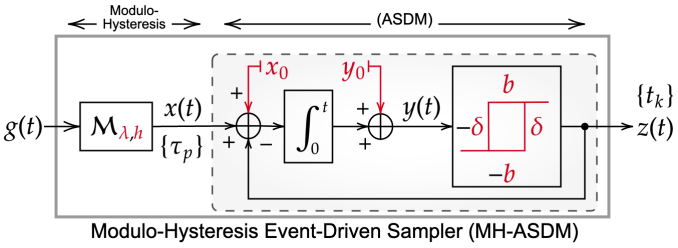

Fig. 1. The proposed high dynamic range event-driven sampler, consisting of a modulo-hysteresis with threshold λ and hysteresis h followed by an asynchronous sigma delta modulator (ASDM). All the design parameters are marked in red ink.

To overcome the DR bottleneck, recently, an alternative sampling protocol has been proposed in the literature, called the Unlimited Sensing Framework (USF) [13–16]. Unlike traditional approaches, the USF follows a *computational sensing* philosophy and leverages a co-design of hardware and algorithms. On the hardware front, modulo non-linearity is inserted before sampling. This ensures that any signal amplitude larger than λ is folded back into the DR of the ADC. In the recovery stage, mathematically guaranteed reconstruction algorithms "unfold" the modulo samples and recover the high dynamic range (HDR) signal [14, 15, 17]. A modulo ADC hardware, namely US-ADC, validating the practical applicability of the USF was recently presented in [15, 18]. A new architecture called *modulo-hysteresis* together with associated recovery guarantees was introduced in [17].

In our ICASSP 2021 paper [12], we took a first step towards combining the benefits of EDS and USF and proposed a **Modulo Event-Driven Sampling (MEDS)** architecture. This included a modulo-hysteresis in series with an integrate-and-fire (IF) EDS model. The IF input has a characteristic lower bound below which no output is generated. By inserting a modulo operation with hysteresis between the input signal and the IF, it was shown that accurate reconstructions can be achieved for signals with higher amplitudes than previously possible [12].

In this work, we bridge the gap between our theoretical results and the practical implementation of the MEDS scheme. We address the problem of identifying a MEDS model comprising a modulo-hysteresis and an asynchronous sigma-delta modulator (ASDM). We will call this model a modulo-hysteresis ASDM sampler (MH-ASDM). The ASDM is an encoding model that was used in continuous-time signal processing [19] and event-driven sampling [2] and is characterized by low-power consumption [20].

Motivation and Contributions. Towards our goal of enabling an end-to-end implementation of the MH-ASDM, we go beyond the

conventional wisdom where event-driven encoder parameters are assumed to be known under *ideal model* assumptions [2]. This motivates the problem of system identification which is particularly relevant in practical scenarios where the hardware may deviate from theoretical design. Furthermore, by identifying the system parameters algorithmically instead of re-designing circuits with different components, we are able to reduce the cost and complexity of hardware implementation and calibration. From an algorithmic standpoint, the MH-ASDM identification is a richer problem than input recovery, because not all ASDM parameters are directly needed for reconstruction [2]. Our key contributions are as follows:

— We formulate the system identification problem in the context of MH-ASDM sampling.

— We present a mathematically guaranteed system identification method using a single input-output signal observation.

— We validate our reconstruction algorithms both in simulations and on a MH-ASDM hardware prototype. Even though hardware design is not the focus of this paper, we developed an MH-ASDM test bed with *off-the-shelf* electronics that incorporates previous implementations of the US-ADC prototype [15, 17].

2. THE MODULO ASDM ENCODER

2.1. The Asynchronous Sigma-Delta Modulator

The ASDM (Fig. 1) consists of a feedback loop containing an adder, an integrator, and a noninverting Schmitt trigger. In the initial time point $t = 0$, the output of the Schmitt trigger is set as $z(t) = -b$. In a vicinity of the $t = 0$ the integrator output $y(t)$ satisfies:

$$y(t) = y_0 + \int_0^t (x(s) + x_0 + b)\, ds, \tag{1}$$

where $x(t)$ is the input, x_0 is the bias, y_0 is the integrator initial condition and b is the Schmitt trigger output voltage, respectively. The ASDM generates output only if $|x(t)| \leqslant c < b$, which implies that $y(t)$ is strictly increasing (1). The spike time t_1 corresponds to $y(t_1) = \delta$, where δ is the Schmitt trigger threshold, which flips the output of the Schmitt trigger to b. This enforces $y(t)$ to be strictly decreasing, and t_2 satisfies $y(t_2) = -\delta$. Generally [2],

$$\int_{t_k}^{t_{k+1}} \left(x(s) + x_0 + (-1)^k b\right) ds = (-1)^k 2\delta. \tag{2}$$

The output is piecewise constant, i.e., $z(t) = (-1)^k b \mathbb{1}_{[t_k, t_{k+1})}$, where $\mathbb{1}_S$ is the indicator function. It was shown that, if $x(t)$ is bandlimited with known bandwidth Ω, then it can be recovered with arbitrary accuracy from sequence $\mathcal{T} = \{t_k\}_{k\in\mathbb{Z}}$ [2].

In the ASDM literature it is generally assumed that the ASDM parameters x_0, δ, b are known. When they are unknown, it is possible to recover only a linear transformation of the input [2], which gives no insight into the encoder functionality. Moreover, if at any point $|x(t)| > b$, then condition (2) is not being met, and thus $t_{k+1} \to \infty$. In practice, the ASDM stops generating an output, thus input recovery is no longer possible (see Fig. 2). The DR limitation of the ASDM is discussed in the next subsection.

2.2. The Modulo-Hysteresis Operator

We will address the ASDM dynamic range in a similar fashion to [12], by inserting a modulo-hysteresis nonlinearity between the input and the ASDM. The modulo-hysteresis operator is defined below.

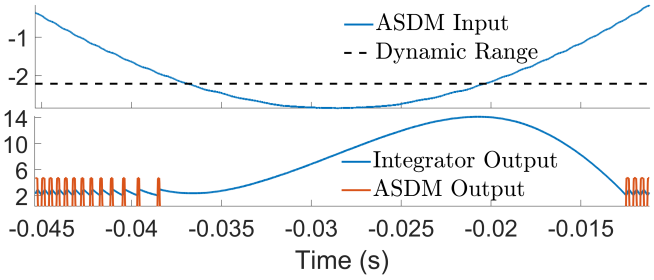

Fig. 2. Output saturation observed in the ASDM hardware prototype.

Definition 1 (Modulo-Hysteresis)**.** *The operator $\mathscr{M}_{\mathbf{H}}$ with threshold λ and hysteresis $h \in [0, \lambda)$, where $\mathbf{H} = [\lambda\ h]$, generates a sequence $\{\tau_r\}$ and a function $x(t)$, $t \geqslant \tau_0$ for bandlimited input g, such that*

$$x(t) = g(t) - \varepsilon_g(t), \tag{3}$$

where $\varepsilon_g(t) = 2\lambda_h \sum_{r\in\mathbb{Z}} s_r \mathbb{1}_{[\tau_r,\infty)}(t)$, $\mathbb{1}_S$ is the indicator function, $\lambda_h \triangleq \lambda - h/2$, $s_r = \operatorname{sign}(g(\tau_r) - g(\tau_{r-1}))$, $r \geqslant 1$, and

$$\tau_1 = \min\{t > \tau_0 | \mathscr{M}_\lambda(g(t) + \lambda) = 0\},$$
$$\tau_{r+1} = \min\{t > \tau_r | \mathscr{M}_\lambda(g(t) - g(\tau_r) + hs_r) = 0\}.$$

We note that, for $h = 0$, $\mathscr{M}_{\mathbf{H}}$ is the ideal modulo [14]. A key property of the modulo-hysteresis model is that, when $h \neq 0$, we can define a minimum distance between any two folding times [12]

$$\tau_{r+1} - \tau_r \geqslant \frac{\min\{h, 2\lambda - h\}}{\Omega g_\infty}, \tag{4}$$

where $g_\infty = \max_t |g(t)|$. The proposed MH-ASDM model is depicted in Fig. 1. The advantages of MEDS for sampling were discussed in [12]. We next discuss the problem of system identification.

3. THE IDENTIFICATION OF A MH-ASDM SAMPLER

When the parameters are unknown, one option is to enforce desired values by precise calibration, performed before each experiment session. An alternative approach proposed in this manuscript is inspired by computational sensing. Specifically, we propose to tackle the parameter identification computationally, which allows using inexpensive hardware with off-the-shelf components with virtually no calibration. In other words, this trades off low hardware complexity for high complexity on the theoretical and computational front.

3.1. Problem Formulation

Given a bandlimited input $g(t)$ and $\{t_k\}$, the proposed problem is to find the MH-ASDM parameters $\{\lambda, h, x_0, y_0, \delta, b\}$. The main difficulty here is that the modulo output $x(t)$ is unknown. Due to the nature of modulo, the MH-ASDM output changes non-linearly with λ. The core idea of the proposed solution exploits that modulo is linear in between the folds and enforces their separation via (4). This will be detailed as follows. Let $\mathcal{L}_k x \triangleq \int_{t_k}^{t_{k+1}} x(s)\, ds$. Then (2)

$$\mathcal{L}_k x = (-1)^k (2\delta - b\Delta t_k) - x_0 \Delta t_k, \tag{5}$$

where $\Delta t_k \triangleq t_{k+1} - t_k$. If the ASDM input is known, the parameters can be inferred directly from (5). However, we assume that $x(t)$ is unknown. If we substitute (3) in (5)

$$\mathcal{L}_k g = \mathcal{L}_k \varepsilon_g + (-1)^k (2\delta - b\Delta t_k) - x_0 \Delta t_k. \tag{6}$$

The unknowns are δ, b, x_0 and $\mathcal{L}_k\varepsilon_g$. However, $\mathcal{L}_k\varepsilon_g$ changes with k, and introduces a new unknown with each equation. To overcome this, we define $K_r \in \mathbb{Z}$ as the indices of the spike right after a fold such that $t_{K_r-1} < \tau_r \leqslant t_{K_r}$. We propose the following assumption

$$\tau_r \leqslant t_{K_r} < t_{K_r+3} \leqslant \tau_{r+1}, \tag{7}$$

for some r. The assumption is motivated by the fact that ε_g is constant in (τ_r, τ_{r+1}). Sufficient conditions for this assumption will be addressed in the next subsection. Then $\varepsilon_g(t_k) = 2N\lambda_h, k \in \{K_r, K_r+1, K_r+2\}, N \in \mathbb{Z}$ (3), and

$$\mathcal{L}_k\varepsilon_g = \int_{t_k}^{t_{k+1}} \varepsilon_g(s)\, ds = 2N\lambda_h \Delta t_k. \tag{8}$$

When substituting (8) in (6), N is an additional unknown, such that

$$2N\lambda_h\Delta t_k + 2(-1)^k \delta - (-1)^k \Delta t_k b - x_0 \Delta t_k = \mathcal{L}_k g. \tag{9}$$

We note that $2N\lambda_h$ and x_0 are dependent in the linear system, as they have the same coefficient, and thus cannot be identified separately from this system alone. We rewrite (9) as

$$x_{0,N}\Delta t_k + 2(-1)^k \delta - (-1)^k \Delta t_k b = \mathcal{L}_k g, \tag{10}$$

for $k \in \{K_r, K_r+1, K_r+2\}$, where $x_{0,N} \triangleq 2N\lambda_h - x_0$. Therefore (10) can be solved uniquely if Δt_k are distinct, which is true in the non-trivial case. To estimate x_0 and λ_h, we assume that (7) holds also for τ_{r+1}, i.e., $\tau_{r+1} \leqslant t_{K_{r+1}} < t_{K_{r+1}+3} \leqslant \tau_{r+2}$. Given that ε_g changes by $\pm 2\lambda_h$ in (τ_r, τ_{r+2}) (3), we have that $\varepsilon_g(t_k) = 2(N+m)\lambda_h, k \in \{K_{r+1}, K_{r+1}+1, K_{r+1}+2\}$, where $m = \pm 1$ is unknown, and thus $x_{0,N+m}$ is identified by solving (10) for these new values of k. Finally, assuming that $x_0 < \lambda_h$

$$\lambda_h = \frac{|x_{0,N} - x_{0,N+m}|}{2}, \tag{11}$$

$$x_0 = 2\lambda_h \left(\left[\!\left[\frac{x_{0,N}}{2\lambda_h} + \frac{1}{2} \right]\!\right] - \frac{1}{2} \right), \tag{12}$$

where $[\![g]\!] = g - \lfloor g \rfloor$ and $\lfloor g \rfloor = \sup\{k \in \mathbb{Z} | \, k \leqslant g\}$ is the floor function. To identify y_0, we make the additional assumption that $g(0) \in [-\lambda + h, \lambda - h]$. Together with (7), it follows that the first spike t_1 is generated before the input is folded, and thus (1)

$$y_0 = \delta - \int_0^{t_1} (g(s) + x_0 + b)\, ds. \tag{13}$$

Finally, to estimate λ, but also to address assumption (7), we require a coarse estimation of the folding times τ_r, unknown before identification, which is addressed in the next subsection.

3.2. Estimation of the Modulo Folding Times

Via direct calculation, (2) can be written independently of δ as

$$\int_{t_k}^{t_{k+2}} x(s)\, ds = -x_0(t_{k+2} - t_k) + b(-1)^k (t_{k+2} - 2t_{k+1} + t_k),$$
$$\frac{1}{t_{k+2}-t_k} \int_{t_k}^{t_{k+2}} x(s)\, ds = -x_0 + b(-1)^k \frac{t_{k+2} - 2t_{k+1} + t_k}{t_{k+2} - t_k}. \tag{14}$$

It can be seen that the expression above can be explained by two subsequences $t_k^i \triangleq t_{2k+i}, i = 0, 1$. Furthermore, we define $X(t) \triangleq \int_0^t x(s)\, ds$. Note that the left-hand side of (14) can be written as $\mathscr{D}X(t_k) \triangleq \frac{X(t_{k+1}^i) - X(t_k^i)}{t_{k+1}^i - t_k^i}$, where $\mathscr{D}$ is the non-uniform difference operator of order 1. For higher orders, we define

$$\mathscr{D}^N f_k = \frac{\mathscr{D}^{N-1} f_{k+1} - \mathscr{D}^{N-1} f_k}{t_{k+N} - t_k}. \tag{15}$$

Operator $\mathscr{D}^N$ was used before for input reconstruction from MEDS data [12]. We have that (14)

$$\tfrac{1}{b}\mathscr{D}^1 X\left(t_k^i\right) = a_k^i - \frac{x_0}{b} \text{ and } \tfrac{1}{b}\mathscr{D}^2 X\left(t_k^i\right) = \frac{a_{k+1}^i - a_k^i}{t_{k+2}^i - t_k^i}, \tag{16}$$

for $\forall i = 0, 1, \forall k \in \mathbb{Z}$, where $a_k^i \triangleq (-1)^i \frac{t_{k+1}^i - 2t_{k+i}^{1-i} + t_k^i}{\Delta t_k^i}$ is independent of the ASDM parameters. Using Definition 1

$$\tfrac{1}{b}\mathscr{D}^2 X\left(t_k^i\right) = \tfrac{1}{b}\mathscr{D}^2 G\left(t_k^i\right) - \tfrac{1}{b}\mathscr{D}^2 E_g\left(t_k^i\right), \tag{17}$$

where $G(t) \triangleq \int_0^t g(s)\, ds$ and $E_g(t) \triangleq \int_0^t \varepsilon_g(s)\, ds$. Given that g is bandlimited, $\left|\mathscr{D}^2 G\left(t_k^i\right)\right| \ll \left|\mathscr{D}^2 E_g\left(t_k^i\right)\right|$ when t_k^i is close to one of the folding times τ_r [12]. Thus the folding times can be detected in reverse order using an appropriately chosen threshold θ as [12]

$$\begin{aligned} K_R &= \max\left\{k \mid \left|\tfrac{1}{b}\mathscr{D}^2 X(t_k)\right| \geqslant \theta\right\}, \\ K_r &= \max\left\{k < K_{r+1} - 3 \mid \left|\tfrac{1}{b}\mathscr{D}^2 X(t_k)\right| \geqslant \theta\right\}, \end{aligned} \tag{18}$$

for $r = R-1, R-2, \ldots, 1$. Equations (18) allow computing t_{K_r} which are right-hand bounds on the folding times τ_r. Then, given that $g(0) \in [-\lambda + h, \lambda - h]$, λ can be estimated as

$$\lambda = g(\tau_1) \approxeq g\left(\tfrac{t_{K_1-1} + t_{K_1}}{2}\right). \tag{19}$$

To guarantee (7), we next need to ensure we have at least 4 spikes between each two consecutive folds. We exploit property (4) of modulo-hysteresis, which yields the following guarantee for (7)

$$\frac{\min\{h, 2\lambda_h\}}{\Omega g_\infty} > 5T_{\mathsf{max}}, \tag{20}$$

where T_{max} is the maximum distance between two spike times, which can be bounded by [2] $T_{\mathsf{max}} \leqslant \frac{2\delta}{b - x_\infty} = \frac{2\delta}{b-\lambda}$. The identification procedure is summarised in Algorithm 1. Our main theoretical result is summarised in the following theorem.

Theorem 1. *Let $\{t_k\}$ denote the spike times triggered by a MH-ASDM model with parameters $\{\lambda, h, x_0, y_0, b, \delta\}$ in response to bandlimited input g. Then the parameters can be uniquely identified from $\{t_k\}$ and $g(t)$ if $x_0 < \lambda_h$, $g(0) \in [-\lambda + h, \lambda - h]$ and*

$$\frac{10\delta}{b - \lambda} \leqslant \frac{\min\{h, 2\lambda_h\}}{\Omega g_\infty}. \tag{21}$$

4. NUMERICAL DEMONSTRATION

To evaluate our estimation results, for a generic parameter p and a spike train $\boldsymbol{\mathcal{T}}$, we define the following error functions

$$\mathsf{Err}_p \triangleq 100\frac{|p - \widetilde{p}|}{|p|}\ (\%) \quad \mathsf{Err}_{\boldsymbol{\mathcal{T}}} \triangleq 100\frac{\|\mathcal{S}_{\widetilde{\boldsymbol{\mathcal{T}}}}(t) - \mathcal{S}_{\boldsymbol{\mathcal{T}}}(t)\|^2}{\|\mathcal{S}_{\widetilde{\boldsymbol{\mathcal{T}}}}(t)\|^2}\ (\%)$$

where $\mathcal{S}_{\boldsymbol{\mathcal{T}}}(t) = \sum_{k\in\mathbb{Z}} e^{-\frac{t-t_k}{C}} 1_{[t_k,\infty)}(t)$ denotes the spike train processed with an exponential filter [21] where constant $C = 10^{-4}$.

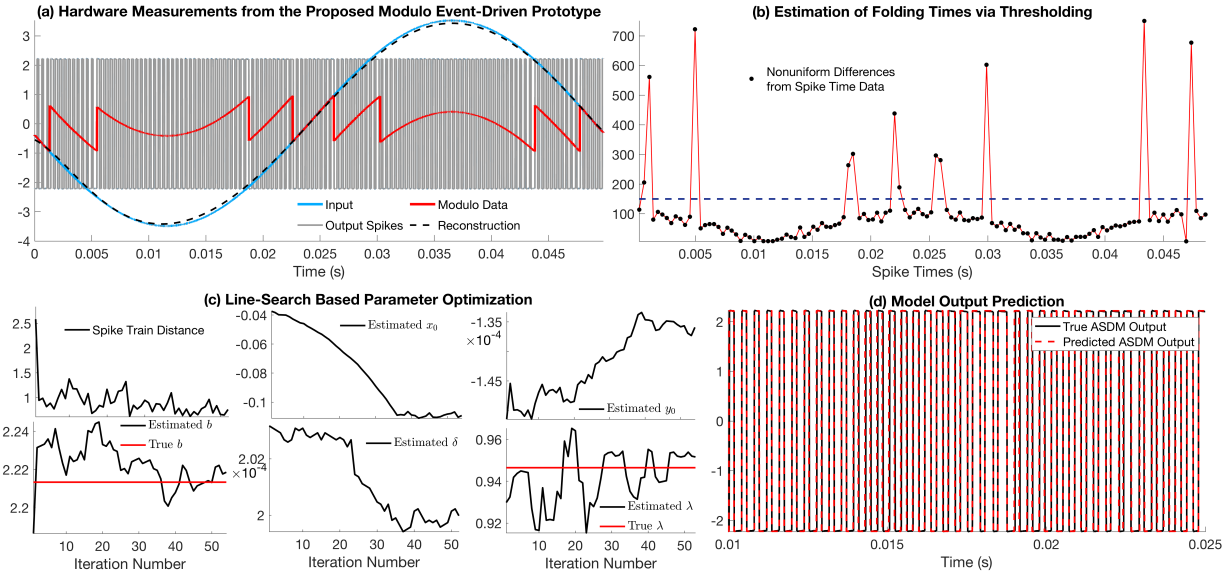

Fig. 3. Hardware Experiment. (a) The input, output of the modulo, the MH-ASDM output spikes, and recovery using estimated parameters. The modulo output is not used for identification. (b) Filtered spike train data and the estimated folding times via thresholding. (c) The analytical parameter estimations are fine tuned with optimization. (d) Proposed model prediction and MH-ASDM prototype output.

Algorithm 1: Identification Algorithm.

Data: $g(t)$ and $\{t_k\}$.
Result: $\lambda, h, b, \delta, x_0, y_0$.

1. Compute subsequences $t_k^i = t_{2k+i}$.
2. Compute $\frac{1}{b}\mathscr{D}^2 X\left(t_k^i\right)$ using (16).
3. Compute $\{K_r\}_{r=1}^R$ with (18).
4. For $r=1$, compute $x_{0,N}, \delta, b$ from (10).
5. For $r=2$, compute $x_{0,N+m}, m \in \{-1,1\}$ from (10).
6. Compute λ_h and x_0 from (12).
7. Compute y_0 with (13).
8. Compute λ with (19) and $h = 2(\lambda - \lambda_h)$.

Identification from Experimental Data. The input is $g(t) = A\sin(\omega(t-\psi))$, where $A = 3.5, \omega = 125$ rad/s, $\psi = 0.024$. We use a MH-ASDM hardware prototype whose parameters are unknown *a priori*. The input $g(t)$, modulo output $x(t)$ and ASDM output $z(t)$ are illustrated in Fig. 3(a). Signal $z(t)$ is first used to estimate λ, h via thresholding [17], purely for validation purposes, as $\lambda = 0.95, h = 0.34$. The spike times $\{t_k\}$, computed from $z(t)$ via zero-crossing, are used to implement Algorithm 1. Steps 2-3 are depicted in Fig. 3(b). The estimated parameters are $\widetilde{x}_0 = -0.11, \widetilde{y}_0 = -1.36, \widetilde{b} = 2.22, \widetilde{\delta} = 1.9 \cdot 10^{-4}$ (for ASDM) and $\widetilde{\lambda} = 0.93$, $\widetilde{h} = 0.32$ (for modulo-hysteresis), with errors $\mathsf{Err}_\lambda = 1.76\%, \mathsf{Err}_h = 2.2\%$. These values were further tuned via numerical optimization using cost function $\mathsf{Err}_{\mathcal{T}}$. At each step, 4 of the parameters $\lambda, b, \delta, x_0, y_0$ were kept constant and the remaining one was optimized via line search over 100 uniformly spaced candidates in a vicinity of radius 4%. The optimization iterates for the remaining 4 parameters, and then the process repeats. The optimization decreases to 0.62% (Fig. 3(c,d)). Finally, we reconstructed the input from $\{t_k\}$ and the estimated parameters via the method in [12] for the equation of our proposed MEDS scheme (6) (Fig. 3(a)).

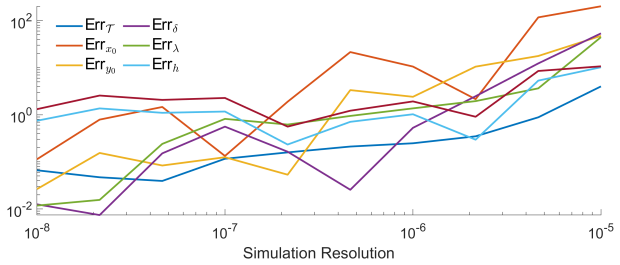

Fig. 4. Analytical computation of the circuit parameters using synthetic data.

Identification from Synthetic Data. In order to validate that the proposed methodology identifies the correct parameters, we run a simulation with synthetic data, where the model is known *a priori*. The input is $g(t) = 2\cdot\sin(600t) - 0.8$, and the model parameters are $\lambda = 0.5, h = 0.25, x_0 = -0.05, y_0 = -2\cdot 10^{-5}, \delta = 5\cdot 10^{-5}, b = 2$. The parameters were then estimated from $g(t)$ and the model response $\{t_k\}$ using Algorithm 1. The errors for all parameters are depicted in Fig. 4 for 10 simulation steps in $\left[10^{-8}, 10^{-5}\right]$. The results show that the errors vanish for a high temporal resolution.

5. CONCLUSIONS

In this work we introduced a new identification routine for a modulo-hysteresis ASDM (MH-ASDM) pipeline. The method is theoretically guaranteed and does not require any information other than the input and MH-ASDM output spike times. We performed hardware experiments to show how the identified model predicts accurately the output of an MH-ASDM hardware prototype. Using synthetic data, we showed how the proposed method identifies the correct parameters. This work is a stepping stone towards enabling the practical functionality of the existing extensive event-driven sampling schemes with HDR inputs.

6. REFERENCES

[1] W. Gerstner, W. M. Kistler, R. Naud, and L. Paninski, *Neuronal dynamics: From single neurons to networks and models of cognition*. Cambridge University Press, 2014.

[2] A. A. Lazar and L. T. Tóth, "Perfect recovery and sensitivity analysis of time encoded bandlimited signals," *IEEE Trans. Circuits Syst. I*, vol. 51, no. 10, pp. 2060–2073, 2004.

[3] A. A. Lazar and E. A. Pnevmatikakis, "Faithful representation of stimuli with a population of integrate-and-fire neurons," *Neural computation*, vol. 20, no. 11, pp. 2715–2744, 2008.

[4] D. Gontier and M. Vetterli, "Sampling based on timing: Time encoding machines on shift-invariant subspaces," *Appl. Comput. Harmon. Anal.*, vol. 36, no. 1, pp. 63–78, 2014.

[5] D. Florescu and D. Coca, "A novel reconstruction framework for time-encoded signals with integrate-and-fire neurons," *Neural computation*, vol. 27, no. 9, pp. 1872–1898, 2015.

[6] R. Alexandru and P. L. Dragotti, "Reconstructing classes of non-bandlimited signals from time encoded information," *IEEE Trans. Sig. Proc.*, vol. 68, pp. 747–763, 2019.

[7] G. Gallego, T. Delbruck, G. M. Orchard, C. Bartolozzi, B. Taba, A. Censi, S. Leutenegger, A. Davison, J. Conradt, K. Daniilidis, and D. Scaramuzza, "Event-based vision: A survey," *IEEE Trans. Pattern Anal. Mach. Intell.*, vol. In Press, pp. 1–26, 2020.

[8] G. G. Gielen, L. Hernandez, and P. Rombouts, "Time-encoding analog-to-digital converters: Bridging the analog gap to advanced digital cmos-part 1: Basic principles," *IEEE Solid-State Circuits Mag.*, vol. 12, no. 2, pp. 47–55, 2020.

[9] M. Miskowicz, *Event-based control and signal processing*. CRC press, 2018.

[10] Y. Tsividis, "Event-driven data acquisition and continuous-time digital signal processing," in *IEEE Custom Integrated Circuits Conference*, 2010, pp. 1–8.

[11] S.-C. Liu, B. Rueckauer, E. Ceolini, A. Huber, and T. Delbruck, "Event-driven sensing for efficient perception: Vision and audition algorithms," *IEEE Signal Process. Mag.*, vol. 36, no. 6, pp. 29–37, 2019.

[12] D. Florescu, F. Krahmer, and A. Bhandari, "Event-driven modulo sampling," in *IEEE Intl. Conf. on Acoustics, Speech and Sig. Proc. (ICASSP)*, 2021.

[13] A. Bhandari, F. Krahmer, and R. Raskar, "On unlimited sampling," in *Intl. Conf. on Sampling Theory and Applications (SampTA)*, 2017, pp. 31–35.

[14] ——, "On unlimited sampling and reconstruction," *IEEE Trans. Sig. Proc.*, pp. 3827–3839, 2021.

[15] A. Bhandari, F. Krahmer, and T. Poskitt, "Unlimited sampling from theory to practice: Fourier-Prony recovery and prototype ADC," *IEEE Trans. Sig. Proc.*, pp. 1–1, Sep. 2021.

[16] A. Bhandari, F. Krahmer, and R. Raskar, "Methods and apparatus for modulo sampling and recovery," 2020, US Patent 10,651,865.

[17] D. Florescu, F. Krahmer, and A. Bhandari, "The surprising benefits of hysteresis in unlimited sampling: Theory, algorithms and experiments," *IEEE Trans. Sig. Proc.*, vol. 70, pp. 616–630, Jan. 2022.

[18] A. Bhandari, "Unlimited sampling with sparse outliers: Experiments with impulsive and jump or reset noise," in *IEEE Intl. Conf. on Acoustics, Speech and Sig. Proc. (ICASSP) (to appear)*, 2022.

[19] N. Tavangaran, D. Brückmann, R. Kokozinski, and K. Konrad, "Continuous time digital systems with asynchronous sigma delta modulation," in *European Sig. Proc. Conf. (EUSIPCO)*, 2012, pp. 225–229.

[20] E. Roza, "Analog-to-digital conversion via duty-cycle modulation," *IEEE Trans. Circuits Syst. II*, vol. 44, no. 11, pp. 907–914, 1997.

[21] W. Maass, T. Natschläger, and H. Markram, "Real-time computing without stable states: A new framework for neural computation based on perturbations," *Neural computation*, vol. 14, no. 11, pp. 2531–2560, 2002.